



Synthesis and properties of tetrathiafulvalenes bearing 6-aryl-1,4-dithiafulvenes

Aya Yoshimura^{1,2}, Hitoshi Kimura¹, Kohei Kagawa¹, Mayuka Yoshioka¹, Toshiki Itou¹, Dhananjayan Vasu³, Takashi Shirahata^{1,2}, Hideki Yorimitsu³ and Yohji Misaki^{*1,2}

Full Research Paper

[Open Access](#)**Address:**

¹Department of Materials Science and Biotechnology, Graduate School of Science and Engineering, Ehime University, 3 Bunkyo-cho, Matsuyama, Ehime 790-8577, Japan, ²Research Unit for Power Generation and Storage Materials, and Research Unit for Development of Organic Superconductors, Ehime University, 3 Bunkyo-cho, Matsuyama, Ehime 790-8577, Japan and ³Department of Chemistry, Graduate School of Science, Kyoto University, Sakyo-ku, Kyoto 606-8502, Japan

Email:

Yohji Misaki* - misaki.yohji.mx@ehime-u.ac.jp

* Corresponding author

Keywords:

cross-conjugated systems; electrochemical properties; extended π -conjugation; digital simulation analysis; tetrathiafulvalene

Beilstein J. Org. Chem. **2020**, *16*, 974–981.

doi:10.3762/bjoc.16.86

Received: 11 February 2020

Accepted: 04 April 2020

Published: 12 May 2020

This article is part of the thematic issue "C–H functionalization for materials science".

Guest Editor: K. Itami

© 2020 Yoshimura et al.; licensee Beilstein-Institut.

License and terms: see end of document.

Abstract

Novel multistage redox tetrathiafulvalenes (TTFs) bearing 6-aryl-1,4-dithiafulvene moieties were synthesized by palladium-catalyzed direct C–H arylation. In the presence of a catalytic amount of Pd(OAc)₂, P(*t*-Bu₃)-HBF₄, and an excess of Cs₂CO₃, the C–H arylation of TTF with several aryl bromides bearing 1,3-dithiol-2-ylidenes took place efficiently to produce the corresponding π -conjugated molecules. We also succeeded in the estimation of the oxidation potentials and number of electrons involved in each oxidation step of the obtained compounds by digital simulations.

Introduction

Tetrathiafulvalenes (TTFs) with extended π -conjugation have attracted attention as possible components of functional materials, such as molecular conductors, field-effect transistors (FETs), and positive electrode materials for rechargeable batteries because the TTF moiety has strong electron-donating properties attributed to the formation of stable aromatic 1,3-dithiol-2-ylidenes (1,3-dithiole rings) by one- and two-electron

oxidation [1-16]. Considerable efforts have been devoted to the development of peripherally benzene- or thiophene-substituted TTFs. As for peripherally benzene-functionalized TTFs, some synthetic approaches, crystal and electronic structures, electrochemical and optical properties, and the nature of radical ion complexes with DDQ or iodine were reported [17-24]. Peripherally thiophene-functionalized TTFs, as potential precursors to

conducting polymers, and organic metals were also prepared and characterized [25–29]. To design more tempting molecules, the attachment of 1,3-dithiole rings to aromatic rings appears very appealing since these allow to produce novel multistage redox systems. However, such molecules could formerly not be synthesized by conventional approaches. In 2011, a breakthrough synthesis of arylated TTF derivatives by a palladium-catalyzed direct C–H arylation was reported, and the structural and electrochemical properties of the products were clarified [30]. This motivated us to synthesize novel multistage redox-TTFs bearing 1,3-dithiole rings on aromatic rings, **1–3** (Figure 1). In addition, we focused on cross-conjugated systems with 1,3-dithiole rings, which are of interest as novel multistage redox systems as well as donor components for organic conductors [1,31–41]. The palladium-catalyzed C–H arylation might offer access to new cross-conjugated molecules bearing vinyl-extended TTF moieties (EBDTs), such as **4** (Figure 1), and the electrochemical properties of these representatives should be brought to light. Herein, we report the synthesis and electrochemical properties of tetrathiafulvalene derivatives **1–4**.

Results and Discussion

Synthesis

First, we tried to synthesize compounds **1** and **2** in one step from pristine TTF and **5**, respectively, through palladium-catalyzed C–H arylation (Table 1). When the aryl bromides **6a,b** were allowed to react with TTF under the conditions A, the products **1a,b** were produced in 46 and 48% yields, respectively (Table 1, entries 1 and 2). Attempted isolations of products **1c** and **1d** failed, despite complete conversions of TTF, because the polarities of the mono-, di-, and triarylated TTFs were extremely close to that of the tetraarylated TTF **1c** and the solubility of these compounds were low and almost beyond isolation for **1d** (Table 1, entries 3 and 4). The palladium-catalyzed C–H arylation of **5** with **6a,b** proceeded to give products **2a,b** in 75 and 86% yields, respectively (Table 1, entries 5 and 6). On the other hand, it was difficult to produce **3** in the same manner because 2-bromothiophenes **7** bearing a 1,3-dithiole ring at the 5-position were unstable, for example, **7a** decomposed at around 41–42 °C (Scheme 1a). Therefore, we achieved the synthesis of **3a** by Pd-catalyzed thienylation of TTF using acetal-protected **8**, followed by deprotection using PTSA·H₂O and

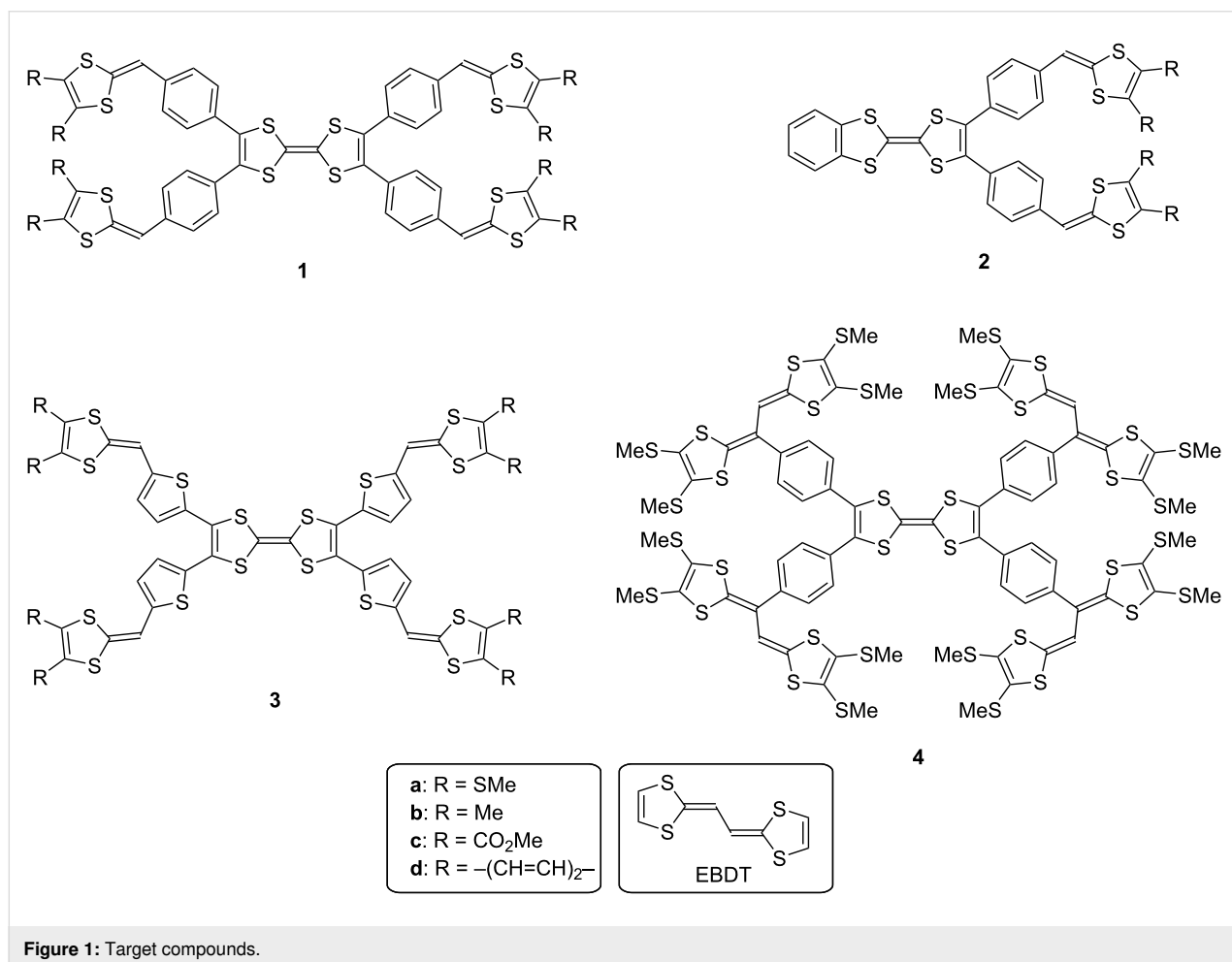
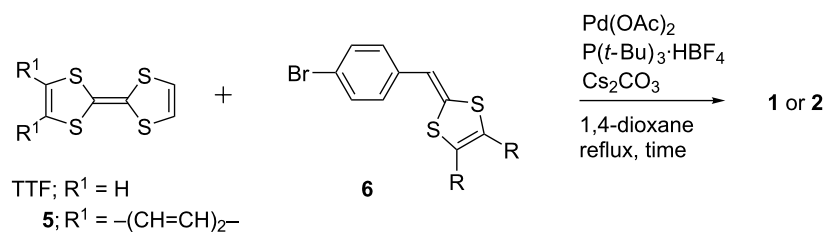


Figure 1: Target compounds.

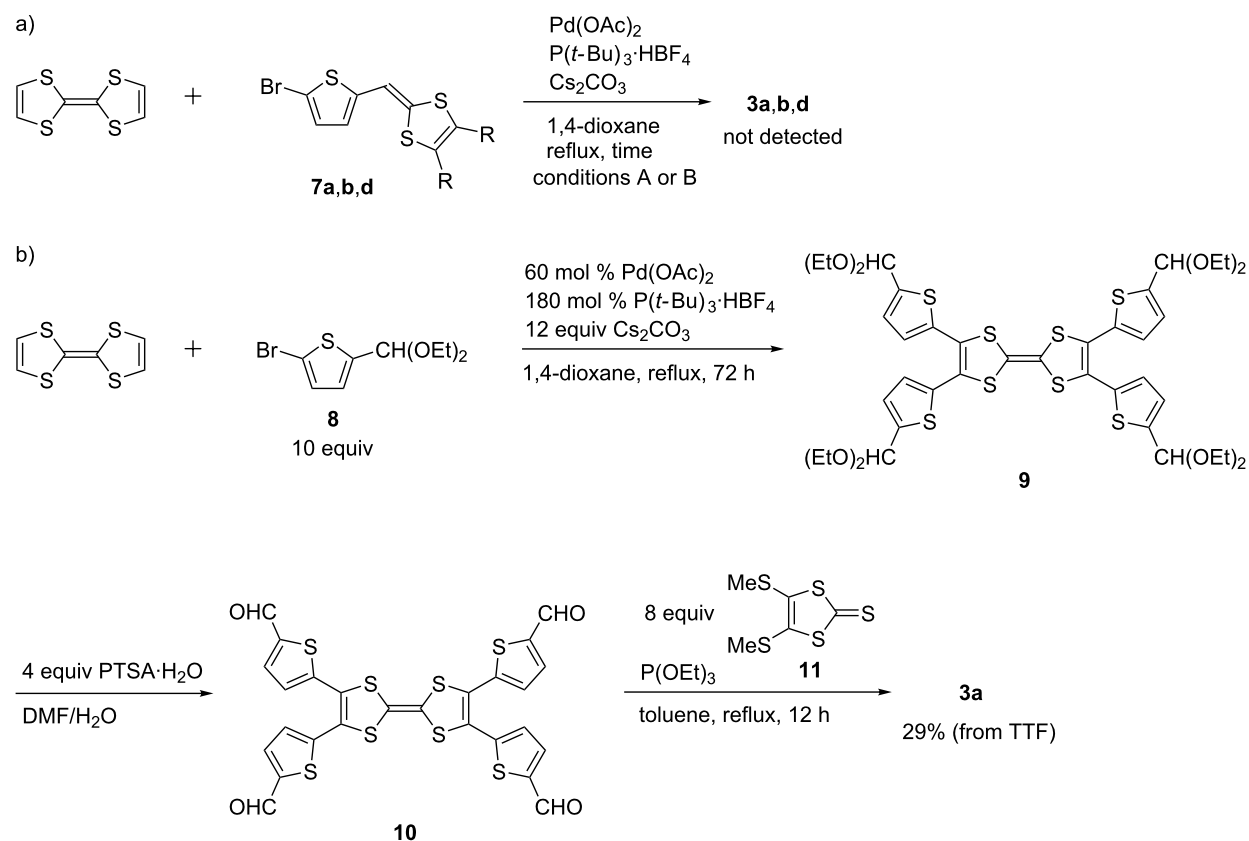
Table 1: Synthesis of compounds **1** and **2**.

conditions A: 30 mol % Pd(OAc)_2 , 90 mol % $\text{P}(t\text{-Bu})_3\cdot\text{HBF}_4$, 6 equiv Cs_2CO_3 , 36 h

B: 60 mol % Pd(OAc)_2 , 180 mol % $\text{P}(t\text{-Bu})_3\cdot\text{HBF}_4$, 12 equiv Cs_2CO_3 , 108 h

entry	TTF or 5	6 (equiv)	conditions	yield of 1 or 2 (%)
1	TTF	6a (5)	A	1a : 46
2	TTF	6b (5)	A	1b : 48
3	TTF	6c (5)	A or B	1c : 0 (mixture)
4	TTF	6d (5)	A or B	1d : 0 (mixture)
5	5	6a (2.5)	A ^a	2a : 75
6	5	6b (2.5)	A ^a	2b : 86

^aReaction time 24 h.

**Scheme 1:** Synthesis of compounds **3**.

P(OEt)₃-mediated cross coupling with **11** (Scheme 1b). The cross-conjugated molecule **4** was prepared in two procedures; one was the palladium-catalyzed C–H arylation of TTF with bromide **12** (Scheme 2a) and the other was the Vilsmeier–Haack reaction of **1a**, followed by triethyl phosphite-mediated cross coupling with **11** (Scheme 2b).

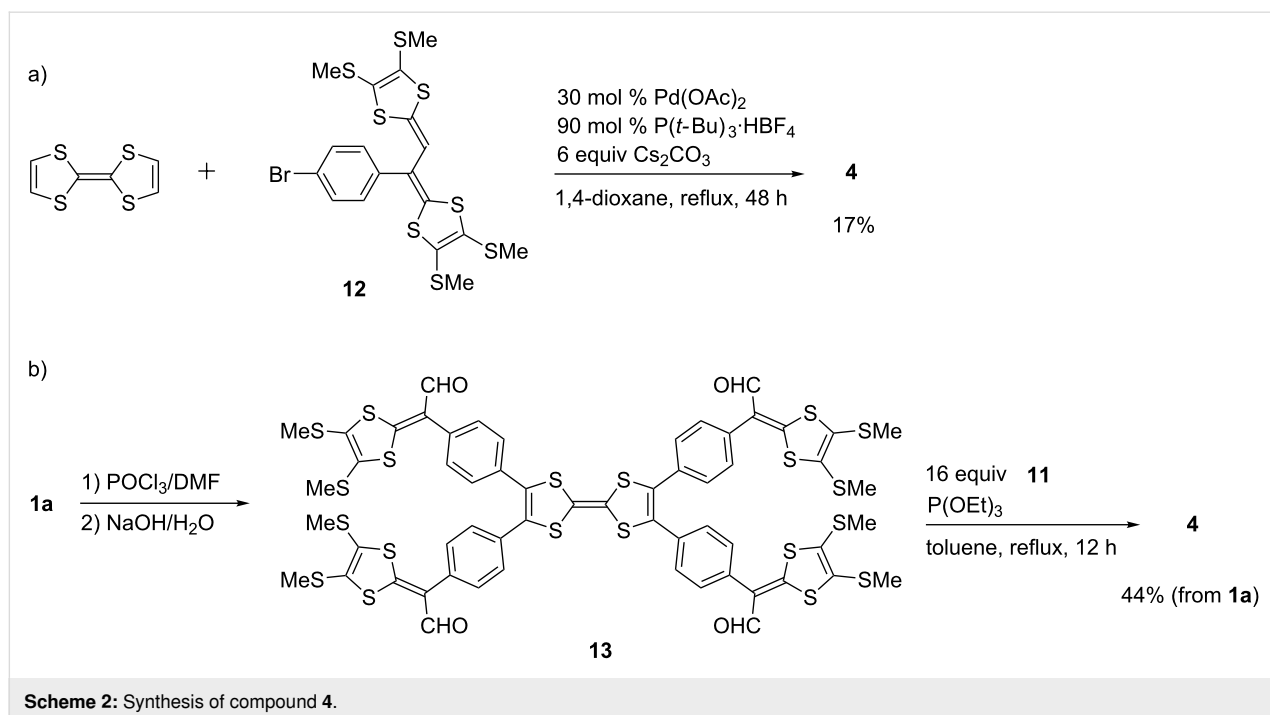
Theoretical calculations

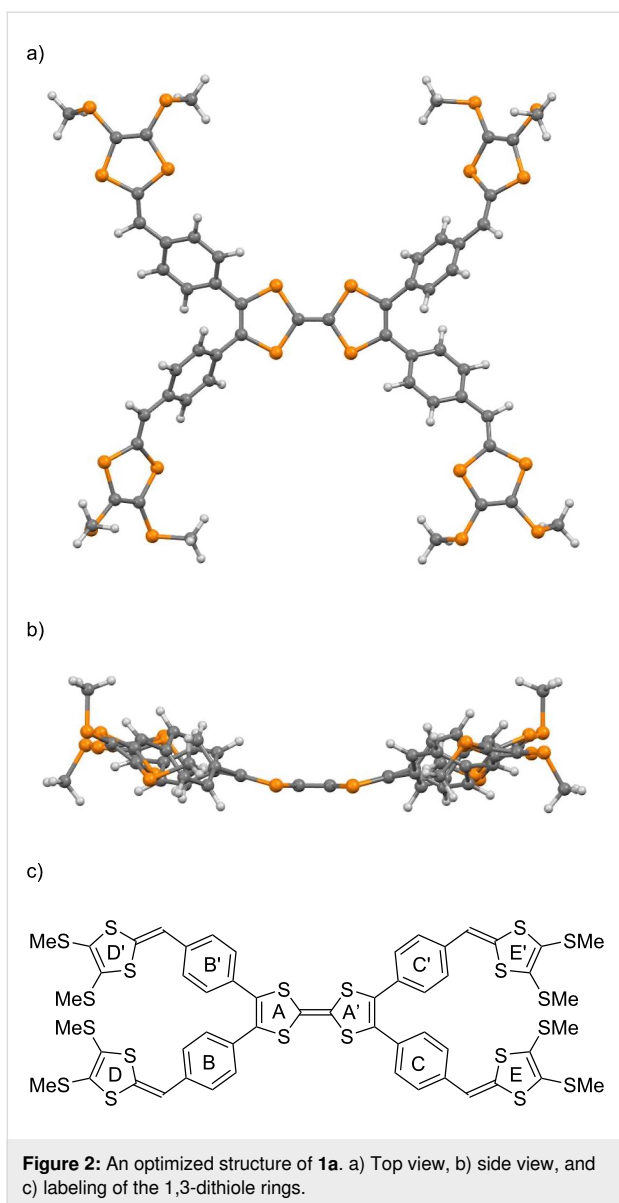
The DFT calculations of compounds **1a**, **3a**, and **4** have been carried out by using the B3LYP/6-31G(d,p) method [42]. Figure 2 shows an optimized geometry of **1a**, and the 1,3-dithiole rings are labeled as A–E and A'–E'. This molecule adopted a nonplanar structure. The angle between the two 1,3-dithiole rings in the center (A–A') was 158.0°. The dihedral angles between A and B, A and B', A' and C, and A' and C' were 49.8°, 137.7°, 137.7°, and 49.9°, respectively. The HOMO, HOMO–1, and LUMO of **1a** are shown in Figure 3. The HOMO of **1a** was mainly located on the TTF moiety, whereas the HOMO–1 was located on the benzene ring and the outer 1,3-dithiole rings at the peripheral part of TTF. The LUMO of **1a** spread over the whole molecule except the outer 1,3-dithiole rings. The orbital energy of the HOMO of **1a** (–4.41 eV) was slightly higher than that of TTF (–4.57 eV). As such, the first oxidation of **1a** might occur at a lower potential than TTF [43].

Cyclic voltammetry analysis

The redox behavior of **1–4** was investigated by cyclic voltammetry. The compounds **1a** and **1b** exhibited four and three pairs

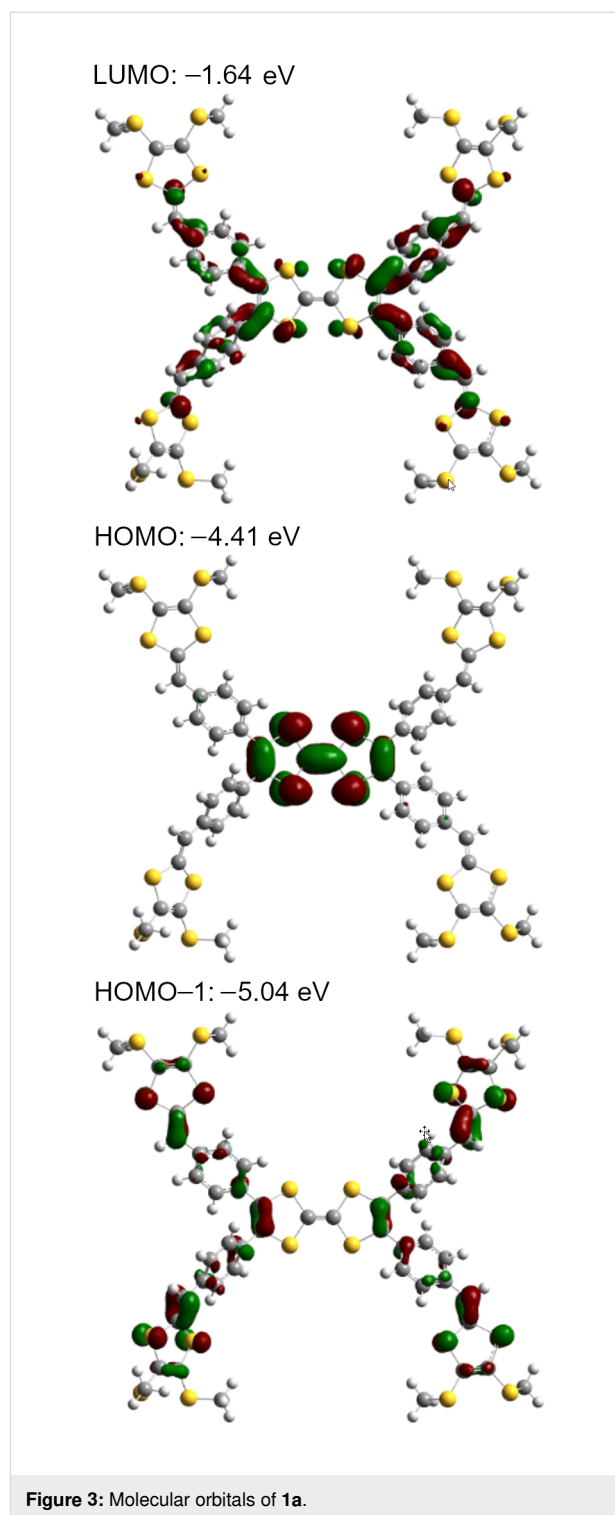
of redox waves, respectively (around +0.03, +0.10, +0.17, and +0.42 V vs Fc/Fc⁺ for **1a** and –0.05, +0.10, and +0.46 V vs Fc/Fc⁺ for **1b**, Figure 4). The redox potentials of **1a,b** are summarized in Table 2 together with the related compound TTF. The redox waves observed at +0.42 V for **1a** and +0.46 V for **1b** were likely related to the second redox of the central TTF moiety because they were close to the E₂ of TTF (+0.37 V). The remaining redox processes observed at around +0.03, +0.10, and +0.17 V for **1a**, and –0.05 and +0.10 V for **1b** might have been derived from the first redox of the central TTF moiety and the redox of the four outer 1,3-dithiole rings. To elaborate the exact oxidation potentials and the number of electrons involved in each oxidation step, a digital simulation technique was applied [44]. As a result, the observed redox waves of **1a** matched the simulated waves (Table 2). It was indicated that the redox wave at +0.10 V was due to an overlap of the sequential two stages of the one- and two-electron transfer waves at +0.07 and +0.12 V, while the other waves corresponded to one-electron transfer processes. The simulation results of **1a** also showed that the redox wave simulated at +0.020 V might have been derived from the central TTF moiety because of the close ΔE values (+0.40 V for **1a** and +0.46 V for TTF). The same discussion was applied to **1b**. In addition, the potentials related to the outer 1,3-dithiole rings of **1a,b** were influenced by the substituents, that is, **1b** bearing electron-donating methyl groups had more negative redox potentials than **1a**. As a consequence, the one-electron redox process of the TTF moiety and the multi-electron redox processes of the outer 1,3-dithiole rings might have overlapped in **1b**.





Compound **2a** exhibited three pairs of redox waves (-0.05 , $+0.09$, and $+0.49$ V vs Fc/Fc^+). The redox waves observed at -0.05 and $+0.49$ V were likely related to the TTF derivative (**5**) moiety, because they were close to the E_1 and E_2 of **5**, respectively (Table 2). The comparison of the peak currents of each wave indicated that the redox wave observed at $+0.09$ V involved a two-electron transfer, while the redox waves observed at -0.05 and $+0.49$ V corresponded to one-electron transfer processes (see the differential pulse voltammetry (DPV) in Supporting Information File 1, Figure S2). These results supported the above-mentioned oxidation potentials and the number of electrons involved in each oxidation step of **1a,b**.

Compound **4** exhibited three pairs of redox waves (around -0.09 , $+0.09$, and $+0.53$ V vs Fc/Fc^+). The redox potentials of **4**



and the simulation results are also summarized in Table 2, together with those of the related compounds TTF and **14** (see Figure 5). The redox process observed at $+0.53$ V was likely related to the second redox of the central TTF moiety because this was the closest to the value of the E_2 of TTF ($+0.37$ V) out of all potentials of the related compounds TTF and **14**. The

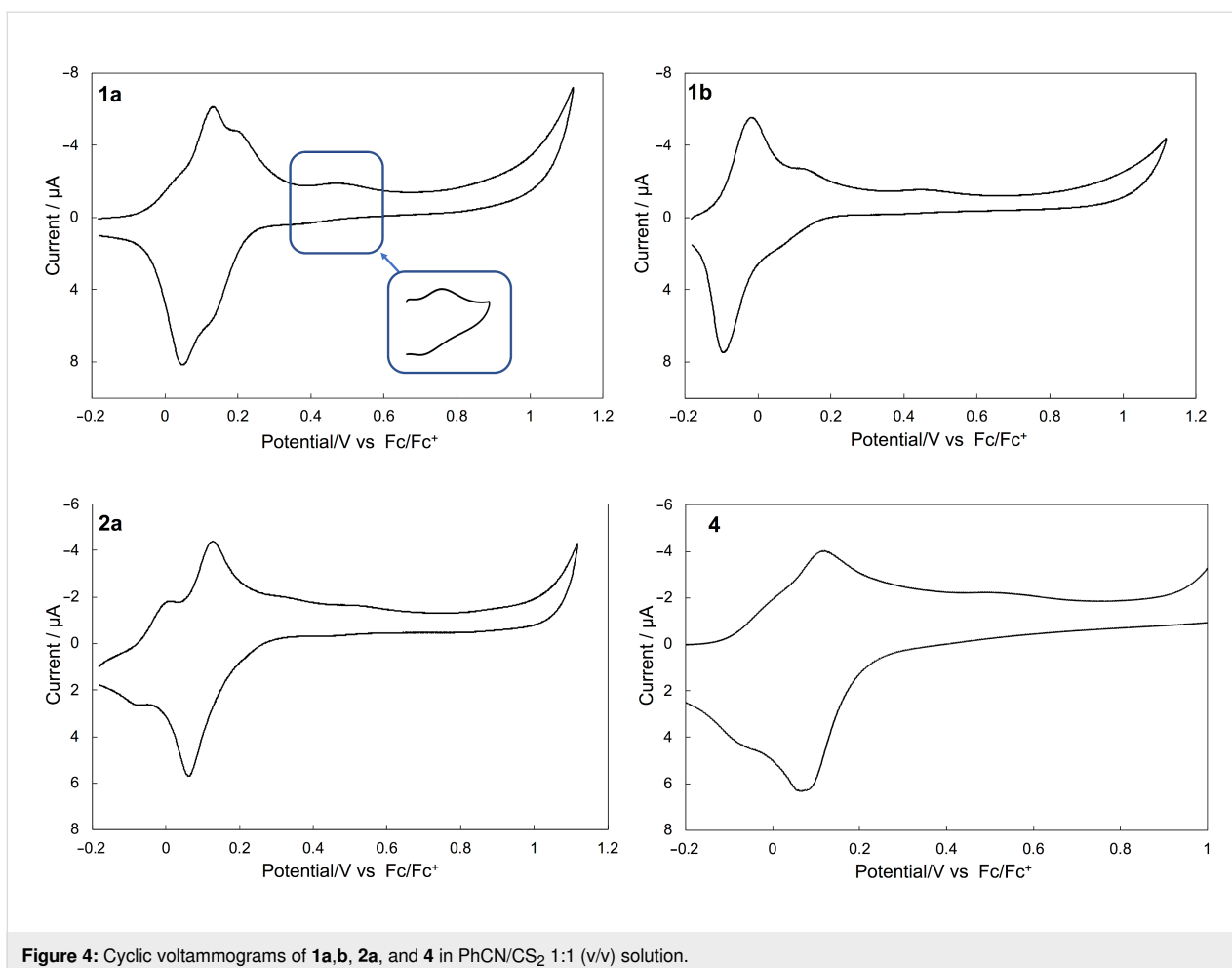


Figure 4: Cyclic voltammograms of **1a**, **1b**, **2a**, and **4** in PhCN/CS₂ 1:1 (v/v) solution.

Table 2: Redox potentials of **1**, **2a**, **4**, and related compounds^a.

compound	observed or simulated value	E_1	E_2	E_3	E_4	E_5	E_6	E_7	E_8	E_9	E_{10}
1a	observed	around +0.03 ^b	+0.10			+0.17	+0.42				
	simulated	+0.020	+0.070	+0.120		+0.200	+0.420				
1b	observed	-0.05				+0.10	+0.46 ^b				
2a	observed	-0.05	+0.09		+0.49						
4	observed	around -0.09			+0.09						+0.53 ^b
	simulated	-0.060	-0.030	+0.010	+0.047	+0.053	+0.098	+0.102	+0.110	+0.180	+0.500
TTF ^c	observed	-0.09	+0.37								
5^c	observed	-0.01	+0.42								
14^c	observed	-0.07	+0.09								

^aIn PhCN/CS₂ 1:1 (v/v) containing 0.1 M *n*-Bu₄NPF₆. ^bAnodic peak. ^cIn PhCN containing 0.1 M *n*-Bu₄NPF₆. All potentials were measured against an Ag/Ag⁺ reference electrode and converted to vs Fc/Fc⁺.

remaining redox processes observed at around -0.09 and +0.09 V might have been due to the first redox of the central TTF moiety, and the overall redox of the EBDT sites, respec-

tively. The observed potentials of **4** were generally consistent with the simulated ones. The results of a digital simulation also showed that the redox wave observed at around -0.09 V and

+0.09 V corresponded to three stages of one-electron transfer and six stages of one-electron transfer processes, respectively. In addition to the overlap of the first redox of the central TTF moiety and the redox of the EBDT sites, each redox potential of the succeeding eight-electron oxidations of the EBDT sites might have slightly shifted due to the non-equivalence of them. Also, the small ΔE value (0.16 V) of **14** caused the redox wave overlap. For these reasons, the first and second redox waves of **4** were broad compared to those of **1a** and **1b**.

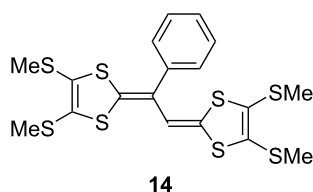


Figure 5: Related compound **14**.

The redox waves of **1a,b** and **4** derived from the second redox of the central TTF moiety (+0.42 V for **1a**, +0.46 V for **1b**, and +0.53 V for **4**) shifted to higher potentials than the second redox of TTF because of the instability of the hexacationic state of **1a,b**, and the decacationic state of **4** compared to the dicationic states of TTF caused by on-site Coulomb repulsion between positive charges in the central TTF moiety and the outer 1,3-dithiole rings. The same discussion could be applied to compounds **2a**. In addition, the observed peak currents of **1a** and **4** in the high potential region at +0.4 to +0.5 V were smaller than those of the simulated waves. This phenomenon might be understood by considering that electron transfer of this redox reaction was slow enough to become the rate-determining step because the crowded structure by which the TTF core is participating in this redox process is surrounded by extended aromatic rings bearing 1,3-dithiol rings.

Conclusion

We have synthesized novel multistage TTF derivatives **1–4** bearing 6-aryl-1,4-dithiafulvene moieties by palladium-catalyzed direct C–H arylation. The DFT calculations revealed the nonplanar structure of the compounds. Cyclic voltammograms of **1a** and **4** comprised four and three pairs of redox waves, respectively. As a result of the digital simulation of **1a**, it was shown that the redox wave observed at +0.10 V involved two stages of one- and two-electron transfer(s), while the other redox waves corresponded to one-electron transfer. The digital simulation of **4** showed 10 stages of one-electron transfer in total. In addition, the first and second redox waves of **4** were broad compared to those of **1** owing to the following three

reasons: a) overlap of the central TTF moiety and the redox of the EBDT sites, b) the succeeding eight-electron oxidations of the non-equivalent EBDT sites, and c) the small ΔE value (0.16 V) of the EBDT sites.

Supporting Information

Supporting Information File 1

Synthetic procedures, theoretical chemical and electrochemical details, and copies of NMR spectra. [https://www.beilstein-journals.org/bjoc/content/supplementary/1860-5397-16-86-S1.pdf]

Funding

This work was partially supported by a Grant-in-Aid for Scientific Research (JP15H03798), from the Ministry of Education, Culture, Sports, Science and Technology (MEXT). This work was also supported by a Grant-in-Aid for Research Promotion, Ehime University, to The Research Unit for Development of Organic Superconductors and to The Research Unit for Power Generation and Storage Materials.

ORCID® iDs

Aya Yoshimura - <https://orcid.org/0000-0001-9967-4598>
 Dhananjayan Vasu - <https://orcid.org/0000-0001-7597-3710>
 Takashi Shirahata - <https://orcid.org/0000-0003-0899-3767>
 Hideki Yorimitsu - <https://orcid.org/0000-0002-0153-1888>
 Yohji Misaki - <https://orcid.org/0000-0002-9079-8487>

Preprint

A non-peer-reviewed version of this article has been previously published as a preprint doi:10.3762/bxiv.2020.16.v1

References

- Yamada, J.; Sugimoto, T., Eds. *TTF Chemistry-Fundamental and Applications of Tetrathiafulvalene*; Kodansha-Springer: Tokyo, 2004.
- Canevet, D.; Sallé, M.; Zhang, G.; Zhang, D.; Zhu, D. *Chem. Commun.* **2009**, 2245–2269. doi:10.1039/b818607n
- Gorgues, A.; Hudhomme, P.; Sallé, M. *Chem. Rev.* **2004**, *104*, 5151–5184. doi:10.1021/cr0306485
- Segura, J. L.; Martín, N. *Angew. Chem., Int. Ed.* **2001**, *40*, 1372–1409. doi:10.1002/1521-3773(20010417)40:8<1372::aid-anie1372>3.0.co;2-i
- Iyoda, M.; Hasegawa, M.; Miyake, Y. *Chem. Rev.* **2004**, *104*, 5085–5114. doi:10.1021/cr030651o
- Hasegawa, M.; Iyoda, M. Tetrathiafulvalene: A Redox Unit for Functional Materials and a Building Block for Supramolecular Self-Assembly. In *Organic Redox Systems*; Nishinaga, T., Ed.; John Wiley & Sons: Hoboken, NJ, USA, 2015; pp 89–129. doi:10.1002/9781118858981.ch4
- Misaki, Y. *Sci. Technol. Adv. Mater.* **2009**, *10*, 024301. doi:10.1088/1468-6996/10/2/024301

8. Inatomi, Y.; Hojo, N.; Yamamoto, T.; Shimada, M.; Watanabe, S. Examination of Multi-Electron Reaction Type pi-Conjugated Organic Compounds as Cathode Active Material for Rechargeable Power Supply. In *ECS Meeting Abstracts, Volume MA2008-01, B1- Batteries General Session, Abstract #167*, 213th ECS meeting, Phoenix, Arizona, May 18–22, 2008; The Electrochemical Society, 2008. doi:10.1149/ma2008-01/5/167
9. Inatomi, Y.; Hojo, N.; Yamamoto, T.; Watanabe, S.-i.; Misaki, Y. *ChemPlusChem* **2012**, *77*, 973–976. doi:10.1002/cplu.201200197
10. Kato, M.; Ogi, D.; Yao, M.; Misaki, Y. *Chem. Lett.* **2013**, *42*, 1556–1558. doi:10.1246/cl.130841
11. Kato, M.; Senoo, K.-i.; Yao, M.; Misaki, Y. *J. Mater. Chem. A* **2014**, *2*, 6747–6754. doi:10.1039/c3ta14920j
12. Iwamoto, S.; Inatomi, Y.; Ogi, D.; Shibayama, S.; Murakami, Y.; Kato, M.; Takahashi, K.; Tanaka, K.; Hojo, N.; Misaki, Y. *Beilstein J. Org. Chem.* **2015**, *11*, 1136–1147. doi:10.3762/bjoc.11.128
13. Yamauchi, T.; Shibata, Y.; Aki, T.; Yoshimura, A.; Yao, M.; Misaki, Y. *Chem. Lett.* **2018**, *47*, 1176–1179. doi:10.1246/cl.180496
14. Ogi, D.; Fujita, Y.; Kato, M.; Yamauchi, T.; Shirahata, T.; Yao, M.; Misaki, Y. *Eur. J. Org. Chem.* **2019**, 2725–2728. doi:10.1002/ejoc.201801877
15. Yamauchi, T.; Kato, M.; Shirahata, T.; Yao, M.; Misaki, Y. *Chem. Lett.* **2019**, *48*, 1507–1510. doi:10.1246/cl.190703
16. Bryce, M. R. *J. Mater. Chem.* **2000**, *10*, 589–598. doi:10.1039/a908385e
17. Coffen, D. L.; Chambers, J. Q.; Williams, D. R.; Garrett, P. E.; Canfield, N. D. *J. Am. Chem. Soc.* **1971**, *93*, 2258–2268. doi:10.1021/ja00738a028
18. Ueno, Y.; Okawara, M. *Chem. Lett.* **1974**, *3*, 1135–1138. doi:10.1246/cl.1974.1135
19. Ueno, Y.; Nakayama, A.; Okawara, M. *J. Am. Chem. Soc.* **1976**, *98*, 7440–7441. doi:10.1021/ja00439a064
20. Yoneda, S.; Kawase, T.; Inaba, M.; Yoshida, Z.-i. *J. Org. Chem.* **1978**, *43*, 595–598. doi:10.1021/jo00398a015
21. Le Coustumer, G.; Mollier, Y. *J. Chem. Soc., Chem. Commun.* **1980**, 38–39. doi:10.1039/c39800000038
22. Babeau, A.; Tinh, N. H.; Gasparoux, H.; Polycarpe, C.; Torreilles, E.; Giral, L. *Mol. Cryst. Liq. Cryst.* **1982**, *72*, 171–176. doi:10.1080/01406568208084054
23. Starodub, V. A.; Baumer, V. N.; Guella, I. M.; Golovkina, I. F.; Alyoshin, V. G.; Nemoskhalenko, V. V.; Senkiewicz, A. I. *Synth. Met.* **1983**, *5*, 101–111. doi:10.1016/0379-6779(83)90124-8
24. Tsujimoto, K.; Okeda, Y.; Ohashi, M. *J. Chem. Soc., Chem. Commun.* **1985**, 1803–1804. doi:10.1039/c39850001803
25. Charlton, A.; Underhill, A. E.; Williams, G.; Kalaji, M.; Murphy, P. J.; Hibbs, D. E.; Hursthouse, M. B.; Malik, K. M. A. *Chem. Commun.* **1996**, 2423–2424. doi:10.1039/cc9960002423
26. Charlton, A.; Underhill, A. E.; Williams, G.; Kalaji, M.; Murphy, P. J.; Malik, K. M. A.; Hursthouse, M. B. *J. Org. Chem.* **1997**, *62*, 3098–3102. doi:10.1021/jo962301q
27. Gompper, R.; Hock, J. *Synth. Met.* **1997**, *84*, 339–340. doi:10.1016/s0379-6779(97)80771-0
28. Zotti, G.; Zecchin, S.; Schiavon, G.; Berlin, A.; Huchet, L.; Roncali, J. *J. Electroanal. Chem.* **2001**, *504*, 64–70. doi:10.1016/s0022-0728(01)00429-6
29. Kakinuma, T.; Kojima, H.; Kawamoto, T.; Mori, T. *J. Mater. Chem. C* **2013**, *1*, 2900–2905. doi:10.1039/c3tc30089g
30. Mitamura, Y.; Yorimitsu, H.; Oshima, K.; Osuka, A. *Chem. Sci.* **2011**, *2*, 2017–2021. doi:10.1039/c1sc00372k
31. Gholami, M.; Tykwinski, R. R. *Chem. Rev.* **2006**, *106*, 4997–5027. doi:10.1021/cr0505573
32. Sugimoto, T.; Awaji, H.; Misaki, Y.; Yoshida, Z.-i.; Kai, Y.; Nakagawa, H.; Kasai, N. *J. Am. Chem. Soc.* **1985**, *107*, 5792–5793. doi:10.1021/ja00306a030
33. Sugimoto, T.; Misaki, Y.; Arai, Y.; Yamamoto, Y.; Yoshida, Z.-i.; Kai, Y.; Kasai, N. *J. Am. Chem. Soc.* **1988**, *110*, 628–629. doi:10.1021/ja00210a069
34. Misaki, Y.; Matsumura, Y.; Sugimoto, T.; Yoshida, Z.-i. *Tetrahedron Lett.* **1989**, *30*, 5289–5292. doi:10.1016/s0040-4039(01)93767-0
35. Amaresh, R. R.; Liu, D.; Konovalova, T.; Lakshmikantham, M. V.; Cava, M. P.; Kispert, L. D. *J. Org. Chem.* **2001**, *66*, 7757–7764. doi:10.1021/jo010663e
36. Rajagopal, D.; Lakshmikantham, M. V.; Cava, M. P. *Org. Lett.* **2002**, *4*, 2581–2583. doi:10.1021/ol026227b
37. Coffin, M. A.; Bryce, M. R.; Batsanov, A. S.; Howard, J. A. K. *J. Chem. Soc., Chem. Commun.* **1993**, 552–554. doi:10.1039/c39930000552
38. Bryce, M. R.; Coffin, M. A.; Skabara, P. J.; Moore, A. J.; Batsanov, A. S.; Howard, J. A. K. *Chem. – Eur. J.* **2000**, *6*, 1955–1962. doi:10.1002/1521-3765(20000602)6:11<1955::aid-chem1955>3.0.co;2-b
39. Hasegawa, M.; Fujioka, A.; Kubo, T.; Honda, T.; Miyamoto, H.; Misaki, Y. *Chem. Lett.* **2008**, *37*, 474–475. doi:10.1246/cl.2008.474
40. Horiuchi, H.; Misaki, Y. *Chem. Lett.* **2010**, *39*, 989–991. doi:10.1246/cl.2010.989
41. Nishiwaki, M.; Tezuka, M.; Shirahata, T.; Misaki, Y. *Chem. Lett.* **2011**, *40*, 467–469. doi:10.1246/cl.2011.467
42. *Gaussian 16*, Revision C.01; Gaussian, Inc.: Wallingford, CT, 2019.
43. The optimized geometries and energy levels of the LUMO, HOMO, and HOMO–1 of **3a** and **4** are shown in Supporting Information File 1, Figure S1.
44. *DigitElch 7 Prof software*; Elchsoft: Kleinromstedt, Germany.

License and Terms

This is an Open Access article under the terms of the Creative Commons Attribution License (<http://creativecommons.org/licenses/by/4.0>). Please note that the reuse, redistribution and reproduction in particular requires that the authors and source are credited.

The license is subject to the *Beilstein Journal of Organic Chemistry* terms and conditions: (<https://www.beilstein-journals.org/bjoc>)

The definitive version of this article is the electronic one which can be found at: doi:10.3762/bjoc.16.86